Available online at www.sciencedirect.com
ScienceDirect
Journal of Molecular Spectroscopy 240 (2006) 112–119
Journal of MOLECULAR SPECTROSCOPY
www.elsevier.com/locate/jms

Infrared emission spectrum of hot D_2O

Nikolai F. Zobov [a,b], Roman I. Ovsannikov [a], Sergei V. Shirin [a], Oleg L. Polyansky [a], Jonathan Tennyson [b,*], Andrew Janka [c,d], Peter F. Bernath [c,d]

[a] Institute of Applied Physics, Russian Academy of Science, Uljanov Street 46, Nizhnii Novgorod 603950, Russia
[b] Department of Physics and Astronomy, University College London, London WC1E 6BT, UK
[c] Department of Chemistry, University of Waterloo, Waterloo, ON, Canada N2L 3G1
[d] Department of Chemistry, University of Arizona, Tucson, AZ 85721, USA

Received 15 July 2006; in revised form 7 September 2006
Available online 15 September 2006

Abstract

An emission spectrum of hot D_2O (1500 °C) has been analyzed in the 2077–4323 cm^{-1} region. A considerable number of new vibration-rotation energy levels have been determined and two new vibrational levels identified. The new (041) and (022) vibrational levels have estimated band origins of 7343.93 ± 0.01 and 7826.38 ± 0.02 cm^{-1}, respectively.

Keywords: Water vapor; Line assignments; Born–Oppenheimer approximation

1. Introduction

The development of a complete theoretical model for the rotation-vibration spectrum of water [1] is an important task because of numerous applications. One of the most difficult aspects to study is the effect of the Born–Oppenheimer approximation on the energy levels [1–4]. Information on deuterated water, D_2O is important for characterizing this effect.

There have been a number of previous studies of the high resolution rotation-vibration spectrum of D_2O [5–14]. These studies have all been performed in absorption using room temperature samples. Until very recently [15–17] there were no reported spectra of hot D_2O. It is hard to characterize excited bending states or states of high rotational excitation, particularly those with high K_a, without studies of hot D_2O. Such states are of particular importance for characterizing the bending region of the potential energy surface which is theoretically the hardest to treat [1,18].

In a paper henceforth referred to as I [15] we reported on a hot (1500 °C) emission spectrum of D_2O recorded in three portions over the 380–1880 cm^{-1} region. This spectrum contained 15,346 emission lines of which we were able to assign 6400 to transitions of D_2O yielding 2144 new rotation-vibration energy levels. As shown below, many of the transitions left unassigned in this spectrum also belong to D_2O. In this present work the range of the emission spectrum is extended to 4323 cm^{-1}.

The spectra in I were analyzed using variational nuclear motion calculations. Given the high accuracy with which it is possible to treat the nuclear motions, the accuracy of such calculations is determined by the accuracy of the underlying potential energy surface and, indeed, the treatment of the Born–Oppenheimer approximation [1,19]. In I we assigned the spectrum iteratively fitting an effective potential energy surface to the energy levels of D_2O. The large number of energy levels determined during the study allowed us to improve significantly this potential and it is this improved effective potential which is used here to analyze the new spectrum. Because of the interconnectedness of the spectrum, we not only report a first analysis of the newly measured 2076–4323 cm^{-1} region but also a

* Corresponding author. Fax: +44 20 7679 7145.
E-mail address: j.tennyson@ucl.ac.uk (J. Tennyson).

0022-2852/$ - see front matter © 2006 Elsevier Inc. All rights reserved.
doi:10.1016/j.jms.2006.09.007

greatly extended analysis of the lower frequency region presented in I.

2. Experiment

The hot D_2O spectra were recorded in September 2001 at the University of Waterloo with a Bruker IFS 120 HR Fourier transform spectrometer. The spectrometer was operated with a CaF_2 beamsplitter and an InSb detector. The spectra reported here in the 1800–4500 cm^{-1} region were recorded using a longwave pass filter at 6666 cm^{-1}; 30 scans were co-added at a resolution of 0.015 cm^{-1}.

A CaF_2 window was used on the emission port of the spectrometer. The water vapor was heated in the center of a 1 m long, 5 cm diameter alumina tube sealed with cooled CaF_2 windows. The tube was placed inside a furnace and heated to 1550 °C, and a slow flow of water vapor was maintained through the cell. The strongest signal and best signal-to-noise ratio was obtained by allowing a small amount of liquid to condense at the base of the window facing the emission port: evaporation under high vacuum maintained a gas pressure of about 20 Torr. The thermal emission from the cell was focused into the emission port of the spectrometer with a parabolic mirror. The lines were measured between 2076 and 4323 cm^{-1} with the WSpectra program of M. Carleer and have an estimated accuracy of 0.001 cm^{-1}. The spectrum was calibrated against a calibrated hot HDO spectrum, which included many D_2O lines in this range.

A sample portion of the spectrum is given in Fig. 1. Table 1 gives assignments to the lines listed in this figure. A full list of the lines recorded in I and in this work has been placed in the electronic archive.

3. Line assignments

As a first step in the analysis of the new D_2O emissions spectrum, it was necessary to remove lines associated with HDO and H_2O. This was done by comparison with hot emission spectra for these species [20–23]. A total of 1005 transitions were identified as belonging to hot H_2O with a further 1072 as belonging to HDO. We note that the hot emission spectrum of HDO ends at 3932 cm^{-1} [23], so we were not able to remove HDO transitions from the highest frequency portion of the spectrum in this fashion.

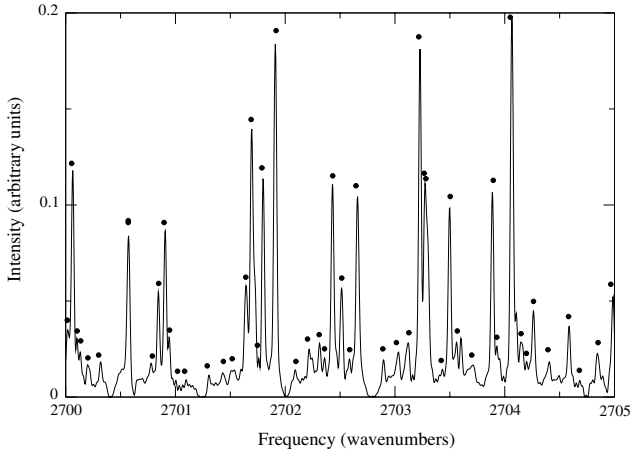

Fig. 1. Section of the D_2O emission spectrum. Lines identified by the dots are listed in Table 1 where assignments are given if available.

The second step in the study involved the identification of those transitions between rotation-vibration states whose energies had already been characterized experimentally. It was possible to make such "trivial" assignments to 8806 lines in the 2076–4323 cm^{-1} region. This left a dataset of just over 15,000 lines in this region to be assigned. These were combined with lines, about 8000 of them, that were left unassigned in the 380–1877 cm^{-1} region in I and analyzed together.

Variational nuclear motion calculations were performed using the Fit 2 potential energy surface presented in I. This fit reproduced an extended dataset of D_2O energy levels with a standard deviation of only 0.033 cm^{-1}. Analysis was based on a linelist which considered all transitions between states with $J \leqslant 30$ and energy less than 14 000 cm^{-1}. Full vibration-rotation quantum number labels were associated with these states using the algorithm of Zobov et al. [25]. See I for further details.

Initial assignments were performed using a semi-automated procedure [24]. This procedure is based on a program which reads the labeled [25] spectrum calculated by the DVR3D nuclear motion program suite [26], the experimental linelist and an energy file comprising experimentally determined energies where available and calculated ones otherwise. Starting from a previously undetermined energy level the program finds all theoretical transitions associated with it. It then tries to match experimental frequencies to these transitions within a given error and then find combination differences within some smaller error, 0.02 cm^{-1} here. These tentative assignments are then manually confirmed or rejected by comparison with the calculated intensities.

Using this procedures a total of 6502 transitions were assigned in the 2076–4323 cm^{-1} region to previously uncharacterized states, similarly 2362 extra transitions were assigned in 380–1877 cm^{-1} region compared to I. These assignments, and the identification of H_2O and HDO lines, have been added to the experimental linelist which covers the whole 380–4323 cm^{-1} region that we have placed in the electronic archive.

4. Analysis

The new assignments presented above can be used to generate further experimental energy levels for the D_2O molecule. Table 2 presents a summary of newly determined energy levels.

The table shows that we have been able to determine new energy levels in 24 different vibrational states and that for most of these states this has also led a significant

Table 1
Line assignments for the spectral region 2700–2705 cm^{-1} given in Fig. 1

Wavenumber (cm^{-1})	Assignment							Comment
	J'	K'_a	K'_c	J''	K''_a	K''_c	$(v'_1v'_2v'_3 - v''_1v''_2v''_3)$	
2700.0225	10	1	9	10	3	8	001–000	t
	26	10	17	26	10	16	001–000	c
2700.0686	14	12	3	14	12	2	011–010	c
2700.1088	9	0	9	9	2	8	001–000	t
2700.1370	8	3	5	8	2	6	100–000	t
2700.2112	22	10	13	22	10	12	011–010	c
	11	4	8	12	1	11	110–010	t
2700.3233	4	1	4	5	1	5	041–040	c
2700.5760	5	1	4	6	1	5	011–010	t
	2	2	0	2	2	1	101–100	t
2700.7799	8	5	4	8	4	5	200–100	t
2700.8491	12	10	3	12	10	2	021–020	c
2700.9108	10	9	1	10	9	2	002–001	c
2700.9492	14	5	10	14	5	9	002–001	c
2701.0076	2	1	2	1	0	1	100–000	t
2701.1211	7	4	4	7	4	3	110–010	HDO
2701.3139	18	11	8	18	11	7	011–010	c
2701.4338	9	2	7	10	1	10	100–000	t
	9	2	8	9	2	7	021–020	t
2701.5275	12	4	8	12	3	9	120–020	c
	8	1	7	7	2	6	200–100	t
2701.6479	9	1	9	9	1	8	001–000	t
	2	1	1	3	1	2	002–001	t
2701.6989	13	12	1	13	12	2	011–010	c
2701.7292	2	2	0	3	2	1	002–001	c
	14	8	7	14	8	6	031–030	c
2701.7627	11	5	7	11	5	6	100–000	HDO
2701.8039	18	13	6	18	13	5	001–000	c
2701.9143	6	0	6	7	0	7	011–010	t
	14	14	1	14	14	0	001–000	n
2702.0977	20	4	16	21	3	19	100–000	t
2702.2308	18	9	10	18	9	9	021–020	c
	24	11	13	24	11	14	001–000	t
2702.3183	3	2	1	3	2	2	101–100	t
2702.3630	3	3	0	4	3	1	031–030	t
2702.4358	11	10	1	11	10	2	021–020	c
	4	1	3	5	1	4	021–020	t
2702.5180	21	12	9	21	12	10	001–000	t
2702.5884	3	3	1	4	3	2	031–030	t
2702.6637	6	1	6	7	1	7	011–010	t
2702.9006	6	5	1	6	5	2	110–010	HDO
	6	3	4	7	4	3	050–030	H_2O
2703.0281	6	3	3	6	2	4	100–000	t
	13	8	5	13	8	6	031–030	c
2703.1198	9	5	5	9	4	6	200–100	t
	6	1	6	6	1	5	031–030	t
2703.2324	12	12	1	12	12	0	011–010	c
2703.2781	5	0	5	6	0	6	021–020	t
2703.3043	17	11	6	17	11	7	011–010	c
2703.4313	7	2	6	6	1	5	200–100	t
2703.5021	5	2	4	6	2	5	011–010	t
2703.5639	2	2	1	3	2	2	002–001	c
	7	2	5	7	1	6	100–000	t
2703.6073								
2703.6946	14	7	7	14	4	10	030–010	t
	1	1	0	2	1	1	012–011	t
2703.8921	10	10	1	10	10	0	021–020	c
2703.9336	17	9	8	17	9	9	021–020	c
	9	8	1	9	7	2	121–021	c
2703.9574								
2704.0698	5	1	5	6	1	6	021–020	t
	17	13	4	17	13	5	001–000	c
2704.1111	13	4	10	14	1	13	100–000	t

Table 1 (*continued*)

Wavenumber (cm^{-1})	Assignment							Comment
	J'	K'_a	K'_c	J''	K''_a	K''_c	$(v'_1v'_2v'_3 - v''_1v''_2v''_3)$	
	1	1	0	1	1	1	101–100	t
2704.1561	10	2	9	10	2	8	011–010	t
2704.2669	12	8	5	12	8	4	031–030	c
	9	0	9	8	1	8	200–100	t
	7	2	6	7	2	5	002–001	t
2704.4063	9	1	9	8	0	8	200–100	t
2704.4945								
2704.5908	5	5	1	5	5	0	022–021	c
	6	2	5	6	2	4	012–011	t
2704.6895	5	5	1	5	5	0	110–010	HDO
2704.8505	5	1	4	5	3	3	011–010	t
2704.8983								
2704.9902	7	7	1	7	7	0	012–011	t

Assignments labelled "t" are trivial and "c" are new assignments confirmed by combination differences; the line labelled "n" is not confirmed. Note the multiple assignments to a single spectral feature.

Table 2
Summary of new energy levels

Vibration level	Band origin	Number of new levels	Highest J	
			Previous	This work
(000)	0.000	2	30	30
(010)	1178.379	91	30	30
(020)	2336.839	226	30	30
(030)	3474.319	342	25	30
(040)	4589.30[a]	63	25	25
(100)	2671.645	144	28	30
(001)	2787.718	184	30	30
(110)	3841.42[a]	417	15	27
(011)	3956.013	499	19	30
(120)	4990.827	135	12	26
(021)	5105.385	302	18	30
(200)	5291.723	54	14	19
(101)	5373.903	123	20	28
(002)	5529.438	332	16	29
(130)	6119.030[a]	36	14	15
(031)	6235.082	160	16	25
(210)	6452.980	4	14	14
(111)	6533.236	48	17	26
(012)	6686.993	128	16	25
(041)	7343.93[a]	184	—	20
(121)	7672.933	75	11	17
(022)	7826.38[a]	127	—	19
(201)	7852.928	27	14	17
(003)	7899.82[a]	66	12	19

Experimental band origins are given in cm^{-1}, those marked [a] are estimates. See Ref. [15] and the text for details.

increase in the range of rotationally excited states for which energies are now available. Indeed for about half of the states analyzed we have doubled or nearly doubled the number of states determined and the range of rotational excitations studied.

In the course of this work we have identified transitions to two previously unobserved vibrational states (041) and (022). Transitions to the 0_{00} level were not observed for either of these states so it is not possible to give a direct empirical determination of their vibrational band origin. However sufficient low-lying rotational states were observed for us to estimate these band origins with considerable confidence using the observed minus calculated differences and our theoretical prediction of the band origin. This gives $7343.93 \pm 0.01\ cm^{-1}$ for the band origin of (041) and 7826.38 ± 0.02 for (022). Conversely for two previously observed vibrational bands, (002) and (012), we were able to assign transitions to the 0_{00} level for the first time and determined the vibrational band origins as 5529.4377 and 6686.9928 cm^{-1}, respectively.

A significant number of newly determined energy levels, a total of 722, belong to the series of bending states (010), (020), (030) and (040), previously analyzed in I. Mikhailenko et al. [17] have shown that there is a strong perturbation at about $K_a = 13$ between the (100) and (020) states. Our previous labeling of the (020) levels was based on intensity considerations and in particular that transitions $J+1 \leftarrow J$ are stronger for pure rotational transitions. The work of Mikhailenko et al., which used effective Hamiltonians, shows that this is not always so. This perturbation also occurs between the (030) and (110) vibrational states. This means that to determine new levels for the (030) state it is also necessary to analyze the (110) state, which was done in the present paper largely using transitions in the (110)–(100), (110)–(010) and (110)–(000) bands. The first band lies in the region of paper I. After then assigning pure rotational and $\Delta v_2 = 1$ transitions between stretching excited vibrational states, which occur in the 380–1877 cm^{-1} region of paper I, it was possible to assign additional transitions to the pure bending states.

Our present analysis almost covers the region spanned by transitions with $\Delta v_2 = 1$ and $\Delta v_3 = 1$, such as (011)–(000). This meant that determining new levels in the (010), (020) and (030) states was important for determining levels in the (021), (031) and (041) states, respectively.

Table 3 presents experimental energy levels for the new vibrational states (041) and (022). A full list of the 3769

Table 3
Energy levels for (041) and (022) vibrational states

J	K_a	K_c	Wavenumber	o–c	
(041)					
2	0	2	7379.6848	−0.02	c
2	1	2	7390.8744	−0.01	c
2	2	1	7440.0142	0.00	c
2	2	0	7440.4364	0.00	c
3	0	3	7414.2503	−0.01	c
3	1	3	7422.4852	0.00	
3	1	2	7439.8789	0.00	c
3	2	2	7476.3040	0.00	
3	2	1	7478.3359	0.00	c
3	3	1	7549.3762	0.00	c
3	3	0	7549.4171	0.00	c
4	0	4	7458.7217	0.00	c
4	1	4	7464.1873	−0.01	c
4	1	3	7492.9173	0.00	c
4	2	3	7524.3478	0.02	c
4	2	2	7530.0328	0.00	c
4	3	2	7599.0118	0.01	c
4	4	1	7696.6003	0.02	dc
4	4	0	7696.6003	0.02	dc
5	0	5	7512.3888	0.00	c
5	1	5	7515.7664	0.00	c
5	1	4	7558.0942	0.00	c
5	2	4	7583.7956	0.01	
5	2	3	7595.8621	−0.01	c
5	3	3	7660.9872	0.01	c
5	3	2	7661.9049	0.01	c
5	4	1	7757.8538	0.01	c
5	5	1	7879.2940	0.02	dc
5	5	0	7879.2940	0.02	dc
6	0	6	7574.9575	0.00	c
6	1	6	7577.0103	0.01	c
6	1	5	7634.5452	0.00	c
6	2	5	7654.3436	0.01	c
6	2	4	7675.7113	0.01	c
6	3	4	7735.2276	0.01	c
6	3	3	7737.7805	0.01	c
6	4	3	7831.4564	0.02	c
6	4	2	7831.5743	0.01	c
6	5	2	7953.0546	0.03	c
6	6	1	8094.7930	0.02	dc
6	6	0	8094.7930	0.02	dc
7	0	7	7646.3990	0.00	c
7	1	6	7721.2813	0.01	c
7	2	6	7735.6843	0.02	c
7	2	5	7768.9914	0.02	c
7	3	5	7821.6282	0.02	c
7	3	4	7827.4193	0.02	c
7	4	4	7917.4784	0.00	c
7	4	3	7917.9256	0.02	c
7	5	2	8039.1964	0.01	
7	6	2	8180.7979	0.01	
7	6	1	8180.9059	0.02	c
8	0	8	7726.7831	0.01	c
8	1	8	7727.2205	0.01	c
8	2	7	7827.7207	0.04	c
8	2	6	7874.9351	0.02	c
8	3	6	7920.0395	0.03	c
8	3	5	7931.2811	0.04	
8	4	5	8015.9232	0.03	c

Difference from the predictions of variational nuclear motion calculations are given as o–c in cm^{-1}. c denotes a level confirmed by combination differences and d set of doubly degenerate levels.

Table 3 (*continued*)

J	K_a	K_c	Wavenumber	o–c	
8	4	4	8017.1201	0.03	c
8	5	4	8137.6871	0.02	c
8	5	3	8137.7521	0.01	c
8	6	3	8280.1503	−0.04	
8	6	2	8279.1633	0.01	
8	8	1	8614.1894	−0.02	dc
8	8	0	8614.1894	−0.02	dc
9	0	9	7816.1787	0.02	c
9	1	9	7816.4197	0.01	c
9	1	8	7922.2924	0.03	c
9	2	8	7933.7102	0.02	c
9	2	7	7992.5903	0.03	c
9	3	7	8030.4909	0.00	c
9	3	6	8049.4462	0.04	c
9	4	6	8126.6557	0.03	c
9	5	4	8248.8168	0.03	c
9	6	3	8389.8128	0.02	c
9	7	3	8550.5522	0.04	
9	8	2	8725.5642	−0.03	d
9	8	1	8725.5642	−0.03	d
9	9	1	8912.6422	−0.07	d
9	9	0	8912.6422	−0.07	d
10	0	10	7914.6085	0.00	
10	1	10	7914.7705	0.04	c
10	1	9	8035.7962	0.03	c
10	2	9	8038.6403	0.04	c
10	2	8	8120.9162	0.03	c
10	3	8	8153.7853	0.03	c
10	3	7	8181.5212	0.03	c
10	4	7	8249.5047	0.02	c
10	5	6	8371.8691	0.01	c
10	5	5	8372.4470	0.02	c
10	6	4	8512.8974	−0.03	c
10	7	4	8673.8982	0.01	dc
10	7	3	8673.8982	0.01	dc
10	8	3	8849.1220	−0.01	dc
10	8	2	8849.1220	−0.01	dc
11	0	11	8022.1691	0.03	c
11	1	11	8022.2457	0.04	c
11	1	10	8157.9891	0.05	c
11	2	10	8159.7302	0.04	c
11	2	9	8258.8693	0.05	c
11	3	8	8326.8035	0.05	c
11	5	7	8507.4977	0.04	
11	5	6	8508.8257	0.03	c
11	6	5	8648.4448	0.01	c
11	7	4	8809.4326	0.01	
12	0	12	8138.7803	0.04	
12	1	12	8138.8431	0.05	c
12	1	11	8288.9546	0.05	c
12	2	11	8289.9903	0.09	c
12	2	10	8405.6708	0.05	c
12	3	9	8484.2539	0.06	c
12	4	8	8561.8320	0.08	c
12	7	5	8957.1854	0.09	c
13	0	13	8264.5126	0.06	c
13	1	13	8264.5452	0.05	c
13	1	12	8428.8606	0.07	c
13	2	12	8429.4756	0.06	c
13	2	11	8560.8118	0.07	c
13	3	11	8567.6369	0.06	c
13	4	9	8728.6381	0.05	c
13	5	9	8815.0791	0.04	c
13	6	8	8958.0613	0.04	c
13	6	7	8956.3201	0.10	

Table 3 (*continued*)

J	K_a	K_c	Wavenumber	o–c	
13	7	7	9116.7703	0.02	c
14	0	14	8399.3200	0.08	c
14	1	14	8399.1951	0.05	c
14	1	13	8577.7422	0.05	c
14	2	13	8578.2878	0.07	c
14	2	12	8725.1727	0.08	c
14	3	12	8729.1435	0.07	c
14	3	11	8831.2707	0.07	
14	4	11	8857.9798	0.06	c
14	4	10	8910.1703	0.06	c
14	5	10	8986.1953	0.06	c
14	6	9	9130.0208	0.06	c
15	0	15	8543.2017	0.08	c
15	1	15	8543.1576	0.05	c
15	1	14	8735.7454	0.08	c
15	2	14	8735.6889	0.07	c
15	2	13	8896.5346	0.08	c
15	3	13	8899.1052	0.08	
15	3	12	9017.5094	0.07	c
15	4	12	9039.1380	0.07	c
15	4	11	9104.8492	0.09	
15	5	11	9172.9490	0.07	
15	6	10	9313.9229	0.07	
15	7	8	9472.8693	0.06	
16	0	16	8696.1575	0.08	dc
16	1	16	8696.1575	0.08	dc
16	1	15	8902.8205	0.09	c
16	2	15	8902.7866	0.09	c
16	2	14	9077.0080	0.09	c
16	3	14	9078.4824	0.10	c
16	3	13	9215.6925	0.08	
16	4	13	9228.6304	0.08	c
16	4	12	9310.9057	0.09	
16	5	12	9366.2807	0.09	c
16	6	11	9509.6071	0.04	
17	0	17	8858.2261	0.06	dc
17	1	17	8858.2261	0.10	dc
17	1	16	9079.0472	0.10	c
17	2	16	9078.9587	0.10	c
17	3	15	9266.9814	0.11	c
17	3	14	9419.5329	0.11	c
17	4	13	9532.1282	0.08	c
17	5	13	9571.6282	0.06	c
17	5	12	9626.3482	0.08	
18	0	18	9029.5173	0.11	c
18	1	18	9029.4448	0.11	c
18	1	17	9264.4504	0.11	c
18	2	17	9264.3006	0.12	c
18	2	16	9464.1529	0.11	c
18	3	16	9464.4490	0.09	c
18	3	15	9631.4719	0.10	
18	4	14	9755.9193	0.11	c
18	5	14	9787.7960	0.11	
18	6	13	9935.6683	0.09	c
19	0	19	9210.6389	0.09	c
19	1	19	9210.2656	0.10	c
19	2	17	9670.3323	0.11	
20	1	20	9396.1950	0.10	c
20	1	19	9663.7170	0.11	c
20	2	19	9662.8404	0.14	c
(022)					
2	1	1	7876.9721	0.06	c
2	2	0	7905.0835	0.07	c
3	0	3	7895.7567	0.06	c
3	1	3	7900.4255	0.07	c
3	1	2	7916.6404	0.07	c
3	3	1	7992.9631	0.07	c
4	0	4	7939.3641	0.06	c
4	1	3	7968.7385	0.06	c
4	2	2	7994.8601	0.06	c
4	3	2	8041.8819	0.08	
4	3	1	8042.2716	0.07	
4	4	1	8113.9959	0.05	dc
4	4	0	8113.9959	0.05	dc
5	1	5	7993.4743	0.07	c
5	2	4	8046.9152	0.07	c
5	3	3	8103.0317	0.09	c
5	4	2	8175.3340	0.05	c
5	5	1	8264.2721	0.07	dc
5	5	0	8264.2721	0.07	dc
6	0	6	8053.7991	0.06	c
6	1	6	8054.4393	0.06	c
6	1	5	8106.6978	0.06	c
6	2	5	8116.4683	0.06	c
6	2	4	8139.9083	0.06	c
6	3	3	8180.8838	0.06	c
6	4	3	8249.2292	0.06	
6	4	2	8249.4488	0.05	c
6	5	2	8338.3814	0.06	dc
6	5	1	8338.3814	0.06	dc
6	6	1	8444.5738	0.06	d
6	6	0	8444.5738	0.06	d
7	0	7	8124.7706	0.06	c
7	1	7	8124.8409	0.07	c
7	1	6	8190.6203	0.07	
7	2	6	8196.4226	0.07	c
7	2	5	8231.7864	0.07	c
7	3	5	8263.3150	0.03	c
7	6	2	8532.5654	0.05	dc
7	6	1	8532.5654	0.05	dc
7	7	1	8653.1857	0.05	dc
7	7	0	8653.1857	0.05	dc
8	0	8	8204.6083	0.05	c
8	1	8	8204.6376	0.06	
8	1	7	8284.2274	0.07	c
8	2	7	8286.4075	0.07	c
8	2	6	8335.1183	0.08	c
8	3	6	8359.2873	0.06	c
8	3	5	8377.2556	0.06	
8	8	1	8888.7657	0.10	dc
8	8	0	8888.7657	0.10	dc
9	0	9	8293.0049	0.07	c
9	1	8	8382.5132	0.06	c
9	2	8	8386.1664	0.09	c
9	2	7	8451.1834	0.10	c
9	3	6	8495.1857	0.05	c
9	4	5	8551.0612	0.09	
9	6	4	8744.0229	0.09	c
9	9	1	9149.5871	0.01	dc
9	9	0	9149.5871	0.01	dc
10	0	10	8391.3414	0.08	c
10	1	10	8391.2743	0.06	c
10	1	9	8493.1355	0.07	c
10	2	8	8573.5600	0.05	c
10	3	8	8584.8712	0.06	c
10	3	7	8626.2918	0.07	c
10	4	7	8668.8078	0.06	c
10	4	6	8679.3359	0.07	c

(*continued on next page*)

Table 3 (*continued*)

J	K_a	K_c	Wavenumber	o–c	
11	0	11	8498.7703	0.07	c
11	1	11	8498.7834	0.08	c
11	1	10	8612.1114	0.08	c
11	2	9	8705.3107	0.07	c
11	3	9	8713.4305	0.07	c
11	3	8	8769.1263	0.05	c
11	4	8	8803.6117	0.07	c
11	4	7	8821.9717	0.07	c
12	0	12	8615.5785	0.06	c
12	1	12	8614.7305	0.06	c
12	1	11	8742.4240	0.06	c
12	2	11	8739.4800	0.06	c
12	2	10	8845.6824	0.07	c
12	3	10	8852.4818	0.07	c
12	3	9	8922.4288	0.06	c
12	4	8	8978.4359	0.07	c
13	0	13	8740.9789	0.06	dc
13	1	13	8740.9789	0.06	dc
13	1	12	8878.6719	0.03	c
13	2	12	8878.6535	0.04	c
13	2	11	8994.6373	0.06	c
13	3	11	9004.4795	0.08	c
13	3	10	9085.1024	0.07	c
13	4	9	9147.7975	0.06	c
14	0	14	8875.8729	0.07	dc
14	1	14	8875.8729	0.07	dc
14	1	13	9025.0597	0.06	c
14	2	12	9152.3403	0.07	c
14	3	12	9150.8872	0.05	c
14	3	11	9256.0232	0.07	c
14	4	10	9328.7729	0.07	c
15	0	15	9019.8793	0.06	dc
15	1	15	9019.8793	0.06	dc
15	1	14	9179.5578	0.03	dc
15	2	14	9179.5578	0.03	dc
15	2	13	9318.9400	0.07	c
15	3	13	9318.1439	0.10	c
15	3	12	9435.0706	0.07	c
16	0	16	9172.9920	0.07	dc
16	1	16	9172.9920	0.07	dc
16	1	15	9343.9773	0.04	dc
16	2	15	9343.9773	0.04	dc
16	2	14	9494.8689	0.07	c
16	3	14	9493.5805	0.05	
16	3	13	9621.9847	0.03	c
16	4	12	9721.3519	0.07	c
16	5	11	9795.0754	0.08	c
17	0	17	9335.2009	0.07	dc
17	1	17	9335.2009	0.07	dc
17	1	16	9517.4722	0.05	dc
17	2	16	9517.4722	0.05	dc
17	3	15	9677.9583	0.03	c
18	0	18	9506.4856	0.07	dc
18	1	18	9506.4856	0.07	dc
18	1	17	9700.0518	0.06	dc
18	2	17	9700.0518	0.06	dc
19	0	19	9686.9501	0.08	dc
19	1	19	9686.9501	0.08	dc
19	1	18	9891.7281	0.05	dc
19	2	18	9891.7281	0.05	dc

energy levels newly determined in this work has been placed in the electronic archive. It is important to consider the uncertainties in these energy levels. For strong, unblended lines the experimental accuracy is in the region of 0.001 cm^{-1}; however, this falls to nearer 0.005 cm^{-1} for the weaker transitions which determine most of our new levels. Combining this uncertainty with possible systematic errors suggests that our new levels are determined with an uncertainty of 0.005–0.01 cm^{-1}.

A second aspect of the error analysis is based on comparison with the results of our variational nuclear motion calculations. For the (041) and (022) states these calculations represent predictions since levels associated with these states were not available for the fits performed in I. Table 3 shows the error in these predictions for each level. These differences are remarkably small, emphasizing the reliability of the D_2O potential determined in I, and show systematic trends suggesting that use of this new data could lead to a further improvement in the potential energy surface.

5. Conclusion

We present an 1500 °C emission spectrum of D_2O recorded in the 2076–4323 cm^{-1} region. The number of transitions recorded is large: 25,803 lines are reported when allowance is made for those transitions which have more than one line assignment. This spectrum is analysed in conjunction with a previously reported [15] D_2O emission spectrum in the 380–1877 cm^{-1} region which covers the higher pure rotational excitations and the v_2 bending bands. This spectrum contains 16,288 lines of which 11,217 had been assigned previously.

Our analysis is based on the use of variational nuclear motion calculations performed using a spectroscopically determined D_2O potential energy surface. We have been able to assign 12,726 D_2O lines in the higher frequency region and a further 2362 lines in the previously reported spectrum. A large number of new energy levels have been determined for D_2O: 3045 here and 5833 in total when the two works are considered together. The majority of these levels have been confirmed using combination differences and, given the demonstrated accuracy of calculations, we are confident that the vast majority of the other levels are also reliable. Altogether this dataset of newly determined energy levels approximately triples the number of known levels for the D_2O molecule. Even with the very large number of lines assigned here, almost 30% of the lines in the two spectra remain unassigned. One can assume that most of these transitions are due to D_2O and therefore these spectra still contain significant extra information.

The analysis presented in this work is based on the use of a spectroscopically determined effective potential energy surface for D_2O. This surface is a combination of the mass-independent Born–Oppenheimer potential energy surface for water and an allowance for mass-dependent effects which arise from failure of the Born–Oppenheimer approximation. Combining this surface with a similar one determined for H_2O, e.g. [27], should yield direct insight into effects beyond the Born–Oppenheimer approximation. So far these surfaces have not been determined from a common

starting point, almost certainly a prerequisite for numerical stability if one is to difference the two surfaces to determine the relatively small Born–Oppenheimer correction terms. This analysis will be the subject of future work.

Acknowledgments

Financial support for this was provided by The Royal Society, INTAS, the NASA astrophysics program, the Canadian Natural Sciences and Engineering Council, the Russian Fund for Fundamental Studies and Leonhard-Euler-Project 05/05887 DAAD. This work was performed as part of IUPAC project number 2004-035-1-100 on "A database of water transitions from experiment and theory".

Appendix A. Supplementary data

Supplementary data for this article are available on ScienceDirect (www.sciencedirect.com) and as part of the Ohio State University Molecular Spectroscopy Archives (http://msa.lib.ohio-state.edu/jmsa_hp.htm).

References

[1] O.L. Polyansky, A.G. Császár, S.V. Shirin, N.F. Zobov, P. Barletta, J. Tennyson, D.W. Schwenke, P.J. Knowles, Science 299 (2003) 539–542.
[2] N.F. Zobov, O.L. Polyansky, C.R. Le Sueur, J. Tennyson, Chem. Phys. Lett. 260 (1996) 381–387.
[3] D.W. Schwenke, J. Phys. Chem. A 105 (2001) 2352–2360.
[4] D.W. Schwenke, J. Chem. Phys. 118 (2003) 6898–6904.
[5] R.A. Toth, J. Mol. Spectrosc. 195 (1999) 98–122.
[6] R.A. Toth, J. Mol. Spectrosc. 162 (1993) 41–54.
[7] S.-M. Hu, O.N. Ulenikov, E.S. Bekhtereva, G.A. Onopenko, S.-G. He, H. Lin, J.-X. Cheng, Q.-S. Zhu, J. Mol. Spectrosc. 212 (2002) 89–95.
[8] O.N. Ulenikov, S.-M. Hu, E.S. Bekhtereva, G.A. Onopenko, S.-G. He, X.-H. Wang, J.-J. Zheng, Q.-S. Zhu, J. Mol. Spectrosc. 210 (2001) 18–27.
[9] J.-J. Zheng, O.N. Ulenikov, G.A. Onopenko, E.S. Bekhtereva, S.-G. He, X.-H. Wang, S.-M. Hu, H. Lin, Q.-S. Zhu, Mol. Phys. 99 (2001) 931–937.
[10] O.N. Ulenikov, S.-G. He, G.A. Onopenko, E.S. Bekhtereva, X.-H. Wang, S.-M. Hu, H. Lin, Q.-S. Zhu, J. Mol. Spectrosc. 204 (2000) 216–225.
[11] X.-H. Wang, O.N. Ulenikov, G.A. Onopenko, E.S. Bekhtereva, S.-G. He, S.-M. Hu, H. Lin, Q.-S. Zhu, J. Mol. Spectrosc. 200 (2000) 25–33.
[12] A.D. Bykov, O.V. Naumenko, L.N. Sinitsa, B.P. Winnewisser, M. Winnewisser, P.S. Ormsby, K.N. Rao, J. Mol. Spectrosc. 166 (1994) 169–175.
[13] A. Bykov, O. Naumenko, L. Sinitsa, B. Voronin, B.P. Winnewisser, J. Mol. Spectrosc. 199 (2000) 158–165.
[14] P.S. Ormsby, K.N. Rao, M. Winnewisser, B.P. Winnewisser, O.V. Naumenko, A.D. Bykov, L.N. Sinitsa, J. Mol. Spectrosc. 158 (1993) 109–130.
[15] S.V. Shirin, N.F. Zobov, O.L. Polyansky, J. Tennyson, T. Parekunnel, P.F. Bernath, J. Chem. Phys. 120 (2004) 206–210.
[16] G. Mellau, S.N. Mikhailenko, E.N. Starikova, S.A. Tashkun, H. Over, Vl.G. Tyuterev, J. Mol. Spectrosc. 224 (2004) 32–60.
[17] S.N. Mikhailenko, G.C. Mellau, E.N. Starikova, S.A. Tashkun, Vl.G. Tyuterev, J. Mol. Spectrosc. 233 (2005) 32–59.
[18] J.S. Kain, O.L. Polyansky, J. Tennyson, Chem. Phys. Lett. 317 (2000) 365–371.
[19] O.L. Polyansky, J. Tennyson, J. Chem. Phys. 110 (1999) 5056–5064.
[20] N.F. Zobov, O.L. Polyansky, J. Tennyson, J.A. Lotoski, P. Colarusso, K.-Q. Zhang, P.F. Bernath, J. Mol. Spectrosc. 193 (1999) 118–136.
[21] N.F. Zobov, O.L. Polyansky, J. Tennyson, S.V. Shirin, R. Nassar, T. Hirao, T. Imajo, P.F. Bernath, L. Wallace, Astrophys. J. 530 (2000) 994–998.
[22] T. Parekunnel, F. Bernath, N.F. Zobov, S.V. Shirin, O.L. Polyansky, J. Tennyson, J. Mol. Spectrosc. 101 (2001) 28–40.
[23] A. Janca, K. Tereszchuk, P.F. Bernath, N.F. Zobov, S.V. Shirin, O.L. Polyansky, J. Tennyson, J. Mol. Spectrosc. 219 (2003) 132–135.
[24] S.V. Shirin, N.F. Zobov, V.A. Savin, O.L. Polyansky, Radiophys. Quant. Electron. 44 (2001) 878.
[25] N.F. Zobov, O.L. Polyansky, V.A. Savin, S.V. Shirin, Atmos. Oceanic Optics 13 (2000) 1024–1028.
[26] J. Tennyson, M.A. Kostin, P. Barletta, G.J. Harris, J. Ramanlal, O.L. Polyansky, N.F. Zobov, Computer Phys. Commun. 163 (2004) 85–116.
[27] S.V. Shirin, O.L. Polyansky, N.F. Zobov, R.I. Ovsyannikov, A.G. Csaszar, J. Tennyson, J. Mol. Spectrosc. 236 (2006) 216–223.